Climate change impacts on mycorrhizae amplify nitrogen limitation on global plant growth

R. K. Braghiere[1,2†], J. B. Fisher[1,2], R. A. Fisher[3,4], M. Shi[1,2], B. S. Steidinger[5], B. N. Sulman[6], N. A. Soudzilovskaia[7], X. Yang[6], J. Liang[8,9], K. G. Peay[5], T. W. Crowther[10], R. P. Phillips[11]

[1]Jet Propulsion Laboratory, California Institute of Technology, 4800 Oak Grove Drive, Pasadena, CA, 91109 USA.

[2]Joint Institute for Regional Earth System Science and Engineering, University of California at Los Angeles, Los Angeles, CA, 90095 USA.

[3]Climate and Global Dynamics Division, National Center for Atmospheric Research, Boulder, CO, USA.

[4]Centre Européen de Recherche et de Formation Avancée en Calcul Scientifique, Toulouse, France

[5]Department of Biology, Stanford University, Stanford, CA, USA.

[6]Environmental Sciences Division and Climate Change Science Institute, Oak Ridge National Laboratory, Oak Ridge, TN, USA.

[7]Environmental Biology Department, Institute of Environmental Sciences, Leiden University, Leiden, The Netherlands.

[8]Department of Forestry and Natural Resources, Purdue University, West Lafayette, IN, USA.

[9]Research Center of Forest Management Engineering of State Forestry and Grassland Administration, Beijing Forestry University, Beijing, China.

[10]Department of Environmental Systems Science, ETH Zürich, Zürich, Switzerland.

[11]Department of Biology, Indiana University, 1001 E Third St, Bloomington, IN 47403, USA.

Corresponding author: Renato K. Braghiere (renato.k.braghiere@jpl.nasa.gov)

† Current address: Jet Propulsion Laboratory, M/S 233-305F, 4800 Oak Grove Drive, Pasadena, CA, 91109 USA.

Key Points:

- Our study suggests that global plant demand for N has increased 25% from 1850 to 2010, while the C costs associated with it have increased 40% in the same period.
- Net Primary Productivity has increase from 40 $PgCyr^{-1}$ in 1850 to 47.5 $PgCyr^{-1}$ in 2010, but the amount of it spent in N acquisition moved from 7.5% to 11.5%.
- Areas of savannas and forest-grasslands transition zones present a higher risk of N limitation to plant growth, which aligns with values of N-fixation peaking.

carbon cost, Community Land Model, Fixation and Uptake of Nitrogen, mycorrhizal fungi, nitrogen uptake, netprimary production

Abstract

Most tree species predominantly associate with a single type of mycorrhizal fungi. Because of the principle differences in mycorrhizal associations, they can differentially affect plant nutrient acquisition and biogeochemical cycling. Here, we use the updated carbon-nitrogen economics within the Community Land Model version 5 (CLM5) to evaluate the impact of mycorrhizal association on the global nitrogen and carbon cycles. Different spatial distributions of plant mycorrhizal associations lead to clear differences in present day Net Primary Productivity by up to 345 ± 21 $TgCyr^{-1}$, owing to the impacts of different symbioses on carbon costs of nitrogen acquisition (4.3% more costly than those originally proposed on average). Simulated global NPP increased throughout the 21st century by 20%, while the carbon costs of nitrogen acquisition have increased at a faster rate by 50%. This suggests that nutrient acquisition will increasingly demand a higher portion of assimilated carbon to support the same productivity.

Plain Language Summary

The majority of plants often join forces with specific types of fungi to improve their nutrient acquisition capacity. Each one of theses different types of fungi can impact nutrient acquisition by plants and ultimately impact globala photosynthesis. In this study, we use the land component of a state-of-the-art Earth System Model to investigate how different spatial representations of fungi-plant interactions across the world impacts the carbon and nitrogen cycles. Our results indicate that due to distinct spatial representations of fungi-plant interactions the difference in global net carbon is 345 ± 21 $TgCyr^{-1}$. This is mainly associated with differences in the amount of carbon spent on nitrogen acquisition (4.3% more than the default version) depending on the fungi-plant association used in the model. Simulated global net carbon increased throughout the 21st century by 20%, while the carbon spent on nitrogen acquisition has increased at a faster rate by 50%. This study suggests that nutrient acquisition by plants will increasingly demand a larger portion of net carbon to support the same photosynthesis.

1 Introduction

Terrestrial ecosystems have been a persistent post-industrial carbon sink, absorbing almost a third of anthropogenic carbon emissions (Ciais et al., 2013; Friedlingstein et al., 2019; Schimel et al., 2015). Studies suggest that terrestrial ecosystem productivity has increased due to elevated CO_2 concentration (Chen et al., 2019; Keenan et al., 2016; Zhu et al., 2016), but it remains unclear whether this will translate to increases in the terrestrial carbon sink in the future (Friedlingstein et al., 2006, 2014; Zhang et al., 2019). It is widely expected that limiting factors such as water (Kolus et al., 2019; Trenberth et al., 2014) and nutrients availability (Fleischer et al., 2019; Terrer et al., 2019; Wieder et al., 2015, 2019; Zaehle et al., 2010) might mediate the responses of terrestrial ecosystems to climate change. Disentangling these mechanisms and exploring the consequences of atmospheric CO_2 increase requires assessment of such mechanisms through Earth System Models (ESMs), which allow comprehensive and spatially explicit assessment of the impacts of future climate on biogeochemical cycles in terrestrial ecosystems.

It has been estimated that as much as 80% of plant nitrogen and phosphorus is provided by fungal root symbionts (van der Heijden et al., 2015), thus it is likely that mycorrhizal associations explain a large fraction of the variance in plant response to elevated CO_2 (Drake et al., 2011; Kivlin et al., 2013; Orwin et al., 2011; Sulman et al., 2017; Terrer et al., 2016, 2018).

However, the global spatial distributions of these mechanisms as well as their potential impacts are still uncertain (Norby et al., 2017; Sulman et al., 2019). Only a handful of ESMs consider mycorrhizal nutrient acquisition when calculating carbon assimilation and allocation (Goll et al., 2017; Wang et al., 2010; Zaehle et al., 2015). The Community Land Model version 5 (CLM5) within the Community Earth System Model (CESM) currently enables an explicit representation of the functional differences between different types of plant symbiotic associations (Brzostek et al., 2014; J. B. Fisher et al., 2010; R. A. Fisher et al., 2019; Lawrence et al., 2019; Shi et al., 2016). However, until recently, one of the major challenges in generating global estimates of nutrient limitation on the global carbon cycle is related to a lack of understanding of the spatial distribution of nutrient-acquiring plant-microbe symbioses. Despite the availability of regional maps of present and past plant symbiotic status (Brundrett, 2017; Jo et al., 2019; Menzel et al., 2016; Swaty et al., 2016), we have only recently begun to develop explicit global data about mycorrhizal and nitrogen fixing associations.

Recently, scientists developed methods for extrapolating spatially sparse measurements into large-scale, spatially explicit maps suitable for applications within ESMs (Shi et al., 2016; Soudzilovskaia et al., 2019; Steidinger et al., 2019; Sulman et al., 2019). These developments for the first time enable examining how mycorrhizal distributions are related to the global carbon and nitrogen cycles. In this study, we seek a better understanding of mycorrhizas on global carbon and nitrogen cycles through incorporating multiple state-of-the-science spatial distributions of mycorrhizal associations in a global ecosystem model. We first compare four existing global data products of global spatial distributions of mycorrhizal associations; Second, we perform transient global runs of CLM5 with increasing CO_2 concentration through the 20th and 21st centuries in order to understand the impact of the CO_2 fertilization effect combined with different spatially variable mycorrhizal representations. Finally, we evaluate the possible impact that a change in spatial mycorrhizal association due to climate change may have on the global carbon cycle.

2 Materials and Methods

2.1 Land Surface Model description: CLM5

CLM5 is the land surface component of CESM2. CLM5 includes three important changes to the representation of plant C and N dynamics: i) the Leaf Utilization of Nitrogen for Assimilation (LUNA) module allows plants to adjust their partitioning of N among the maximum rate of carboxylation (V_{cmax}), the maximum rate of electron transport (J_{max}), and other leaf N components, to achieve co-limitation of photosynthesis under the prevailing time-averaged environmental drivers (CO_2, temperature, humidity, soil moisture, radiation, and day length) (Ali et al., 2016; R. A. Fisher et al., 2019; Xu et al., 2012); ii) the 'FlexCN' module allows plants to alter and optimize their stoichiometry, removing the down- regulation of gross primary productivity (GPP) that was used in CLM4 and CLM4.5 (Cheng et al., 2019; Ghimire et al., 2016). In the new allocation algorithm, the total nitrogen supply in each timestep is partitioned among tissues in proportion to their relative 'demand' terms. Additional details on how stoichiometry is optimized can be found in Lawrence et al. (2019) and Fisher et al. (2019); iii) the Fixation and Uptake of Nitrogen (FUN) module implements a 'carbon cost' for each source of plant nitrogen uptake - symbiotic N fixation, uptake of soil N, and retranslocation from leaves (Allen et al., 2020; Brzostek et al., 2014; Fisher et al., 2010; Shi et al., 2016). Plants shift uptake pathways to minimize the costs of N uptake, and also modify tissue C:N allometries in

response to the changing cost of N acquisition (Fisher et al., 2019). Carbon costs of N uptake are added to plant autotrophic respiration. FUN simulates uptake from the two major types of fungi that plants associate with: arbuscular mycorrhizal (AM) or ectomycorrhizal (ECM) fungi. Explicit representation of mycorrhizal associations improved the dynamic predictions of the N retranslocated from leaves and taken up from the soil in a previous ecosystem-scale study (Brzostek et al., 2014).

The cost of N uptake from soil by mycorrhizal or non-mycorrhizal pathways, for each soil layer j, is controlled by two uptake parameters that pertain respectively to the relationship between soil N content and N uptake, and between fine root C density and N uptake. For mycorrhizal or non-mycorrhizal N uptake the cost functions are given as:

$$N_{cost,pathway,j} = \frac{k_{n,pathway}}{N_{smin,j}} + \frac{k_{c,pathway}}{c_{root,j}} \quad (1.0)$$

where $k_{n,\text{pathway}}$ and $k_{\text{c,pathway}}$ varies according to whether the pathway considered is referring to a non-mycorrhizal, an ecto, or an arbuscular mycorrhizal uptake. $N_{smin,j}$ and $c_{root,j}$ are the soil N content ($gN.m^{-3}$) and fine root C density ($gC.m^{-3}$), respectively. Please refer to ref. (NCAR, 2019) for the complete set of equations.

In order to generate the trade-offs between AM, ECM, and non-mycorrhizal root uptake, FUN uses an estimate of the percentage of aboveground biomass per pixel that associates with each mycorrhizal type for each model grid cell (Brzostek et al., 2014). To do so, ref. (Shi et al., 2016) classified the PFTs in CLM, based upon known associations between plant species and either AM- or ECM-fungi described in the literature(E. B. Allen et al., 1995; Phillips et al., 2013; Read, 1991) and these estimates are retained as the default in CLM5. While some PFTs are usually AM-dominated (e.g., grasslands), others are usually ECM-dominated (e.g., boreal forest). However, the assumptions of PFT fractions of mycorrhizal associations are coarse and do not capture the spatial heterogeneity that is observed across the landscape(Shi et al., 2016), particularly in mixed-mycorrhizal PFTs, such as tropical(Waring et al., 2016) and temperate forests (Phillips et al., 2013).

PFT symbiont fraction estimates are available as ratios of the AM-associated and ECM-associated plants of the CLM PFTs as a table in ref. (Shi et al., 2016). These numbers are usually binary, associating one PFT with a single type of mycorrhizae, e.g., 0% or 100%, except for broadleaf deciduous temperate trees, which associates 50% with AM and 50% with ECM. By doing so, the authors indirectly related mycorrhizal associations with climate variables, because the input map of PFTs spatial distribution is mostly driven by climate (temperature, humidity, and radiation) and topography (elevation).

2.2 Coupling mycorrhizae spatial distribution into CLM5

PFTs are used to classify plants according to their physical, phylogenetic, and phenological characteristics. In the CLM5, within each grid cell, the soil area available for vegetation is divided into patches that correspond to the areal fraction of that PFT. For each PFT, a number of key parameters are defined, such as the target tissue C:N values, stomatal water use efficiency, maximum hydraulic conductivity and sensitivity to embolism (see ref. (Kennedy et al., 2019), tissue allocation fractions (for leaves, fine roots, stem, and coarse roots),

tissue turnover times, and the rate at which litter class (labile, lignin, cellulose) decays and returns nutrients to the soil after death. The value of each parameter is where possible determined or inferred from observable characteristics.

A spatial data product can be simply added as a 2D variable varying as function of latitude and longitude, but because land surface models also work with the concept of PFTs, adding a third dimension (i.e., latitude, longitude, PFT) into the spatial distribution can improve accuracy of processes and model uncertainty (Braghiere et al., 2019). Here, given new datasets of spatial distributions of mycorrhizal associations based on observations at different spatial resolutions, we evaluate the impact of this new level of information to nutrients uptake and the global carbon cycle calculated by CLM5.

Four global maps of mycorrhizal association based on different assumptions and spatial resolutions were used to provide the percentage of ectomycorrhizal association (relative to arbuscular mycorrhizal) data for CLM5: Map A (ref. (Shi et al., 2016)); Map B (ref. (Sulman et al., 2019)), Map C (ref. (Steidinger et al., 2019)), and Map D (ref. (Soudzilovskaia et al., 2019)).

Ref. (Sulman et al., 2019) assembled empirical AM data points presenting species number of AM fungi obtained from the MAARJAM database(Öpik et al., 2010), and ECM data points presenting species number of ECM fungi obtained from ref. (Tedersoo et al., 2014). These data were used to define niche models which were used to develop spatial maps of the relative probability of AM and ECM fungal presence within areal units of 10 arcmin. These niche models were used to estimate %ECM by comparing the relative probability of AM and ECM presence: %ECM = 100*p(ECM)/(p(ECM) + p(AM)) where p(ECM) and p(AM) are the probabilities of ECM or AM presence, respectively, from the niche model in each grid cell.

Ref. (Steidinger et al., 2019) proposed a global map of the symbiotic status of forests, using a database of over 1 million forest inventory plots containing more than 28,000 tree species, and 70 global predictor layers: 19 climatic indices (relating to annual, monthly, and quarterly temperature and precipitation variables), 14 soil chemical indices (relating to soil nitrogen density, microbial nitrogen, C:N ratios and soil P fractions, pH and cation exchange capacity), 26 vegetative indices (relating to leaf area index, total stem density, enhanced vegetation index means and variances), and 5 topographic variables (relating to elevation and hillshade). Their maps provide quantitative estimates of the distribution of aboveground biomass fractions among AM, ECM, and N fixers plants within areal units of 0.5° and 1.0°.

Ref. (Soudzilovskaia et al., 2019) assembled a global database on plant mycorrhizal type associations that included 2,169 studies and 27,736 species-by-site records for 12,702 plant species and combined it with information about dominant plant species and their growth form across distinct combinations of Bailey's with 98 ecoregions(Bailey, 2014) and European Space Agency (ESA) landcover categories(ESA, 2017) with spatial resolution of 300 m. Their maps provide quantitative estimates of the distribution of aboveground biomass fractions among AM, ECM and ericoid mycorrhiza (ERM) plants within areal units of 10 arcmin.

The map of ref. (Soudzilovskaia et al., 2019) and the map of ref. (Sulman et al., 2019) are principally different from that of ref. (Steidinger et al., 2019) and ref. (Shi et al., 2016). Consequently, conversions to unify the data for comparisons have to be applied. The map of ref. (Soudzilovskaia et al., 2019) shows fractions of biomass for all plans, not only trees, while the map of ref. (Sulman et al., 2019) shows the likelihood of occurrence of ectomycorrhizal biomass in a grid cell based on a species distribution model fit to a genomic database. Ref. (Sulman et al.,

2019) produced a range from very low likelihood of ECM fungal DNA being present in observations to higher likelihood of ECM presence. In order to compare ref. (Sulman et al., 2019) map with other maps, the ECM map was first combined with the AM map and normalized, producing a spectrum that incorporates both mycorrhizal types.

A regridding process of the maps to CLM5 grid scales was applied by calculating an average value for ECM in percentage per PFT per gridcell based on the GLC2000 land cover data(Bartholomé & Belward, 2005) at a spatial resolution of 500 m following a look-up table (**Supplementary Table S1**). The average value of ECM percentage was assigned to one of the 16 particular natural vegetation PFTs in CLM5 per gridcell, assuming that AM and ECM trees do not differ in biomass. In this case, using basal area maps and biomass percentages map interchangeably is acceptable in tree-dominated areas. In other areas, it is assumed that although differences in the data products might exist, the nature of the measure is assumed to have little impact, as long as given in the format of a ratio of ECM over ECM plus AM present in the gridcells, due to the fact that CLM5 ingests the data as a ECM ratio per PFT.

2.3 Simulation protocols

First, for each ectomycorrhizal percentage map, initial ecosystem C and N stocks for 1850 were generated using a spin-up approach where we ran the model using 1850 concentrations of CO_2 (284.7 ppm) and the model's standard climate forcing dataset from the Global Soil Wetness Project Phase 3 version 1 (GSWP3v1)(Kim, 2017) at 1.9° x 2.5° spatial resolution. The Model for Scale Adaptive River Transport (MOSART) was turned on and ice evolution on land was turned off. The model ran with biogeochemistry mode on without crops for 200 years in 'accelerated decomposition' mode (see ref. (Lawrence et al., 2019) for details) by cycling through the 1901–1920 climate forcing dataset and then for 400 years in regular mode until soil and plant C and N stocks achieved steady state. Following that, we ran a historical simulation from 1850 to 2010 using transient GSWP3 climate, N deposition, and variable atmospheric CO_2 concentration.

Second, in order to illustrate the sensitivity of the model to changes in global patterns of tree symbiosis under climate change, we used a projected map of symbiotic status of forests for 2070 using a relative concentration pathway (RCP) of 8.5 $W.m^{-2}$ and the same relationships observed for current climates from ref. (Steidinger et al., 2019) versus the original map with present climate per PFT per gridcell as in ref. (Steidinger et al., 2019). The projected map suggests that the abundance of ectomycorrhizal trees will decline by as much as 10%, which corroborates the results of common garden transfer and simulated warming(Peter B. Reich et al., 2015) experiments.

We performed 55 years (2015-2070) offline run with the biogeochemistry mode on following the Shared Socio-Economic Pathway (SSP) number 5(Kriegler et al., 2017). SSP5 scenarios are the only ones resulting in a radiative forcing pathway as high as the highest RCP8.5 used by ref. (Steidinger et al., 2019). SSPs are used as inputs for the latest ESMs to explore how societal choices will affect greenhouse gas emissions and, therefore, how the climate change mitigation goals could be met(Riahi et al., 2017). The SSP5 scenarios include extreme levels of fossil fuel use, up to a doubling of global food demand, and up to a tripling of energy demand and greenhouse gas emissions over the course of the century, marking the upper end of the scenario literature in several dimensions. The climatological forcing is from of a CESM simulation from the CMIP6(Lawrence et al., 2016; O'Neill et al., 2016). CLM5 was run globally

at a 1.9 x 2.5 degree spatial resolution with the present and projected maps of ectomycorrhizal symbiotic status of ref. (Steidinger et al., 2019).

We used the LMWG diagnostics package from NCAR (http://github.com/NCAR/CESM_postprocessing) to compare each one the updated runs with those using the PFT look-up table for ectomycorrhizal-fraction used in the default CLM5.

2.4 Calculating nitrogen limitation

The risk of nitrogen limitation (NL) is calculated as:

$$NL = 1. - \frac{\propto_1(i,j)}{\propto_2(i,j)} \quad (2.0)$$

where α_1 is the slope of the linear regression of NPP used for Nitrogen uptake per gridcell (NPP_NUPTAKE(i,j)) with time and α_2 is the slope of the linear regression of NPP (NPP(i,j)) plus NPP_NUPTAKE(i,j) with time. Areas in red indicate higher risk of nitrogen limitation on NPP based on the period from 1850 to 2010.

3 Results

3.1 Different estimates of plant symbiotic status

The two major types of fungi that plants commonly associate with are arbuscular mycorrhizal (AM) and ectomycorrhizal (ECM) fungi. A transition from AM to ECM dominance was observed at site level experiments usually following a transition from phosphorus to nitrogen limitation of plant growth along with increasing latitude(McGroddy et al., 2004b; P. B. Reich & Oleksyn, 2004). The four data products representing the global spatial distribution of the fraction of ECM (relative to AM) associations are shown in **Fig. 1**. These four maps were generated using different methodologies and datasets, and a detailed description of each map is given in **Methods**.

The concept of Map A was generated by associating one type of mycorrhizae to specific Plant Functional Types (PFTs) following previously documented geographic distributions of plant symbiosis(E. B. Allen et al., 1995; Read, 1991). Map A (**Fig. 1a)** was determined from default configuration used in the CLM5, and was here derived by multiplying the ratios of ECM-associated plants in CLM5 PFTs described in in ref. (Shi et al., 2016) by the PFT distribution in CLM5(Lawrence et al., 2019). **Fig. 1a** has binary values with most of the tropics having 0% of fraction of ECM and the boreal regions having 100% fraction of ECM.

The Map B (**Fig. 1b)** was derived from a database containing AM DNA sequence data originated from ecological studies based on *in-situ* or cultured fungi samples(Öpik et al., 2010). The Map C (**Fig. 1c)** was derived from a machine learning technique referred to as 'random-forest' trained with a database of over 1 million forest inventory plots and 70 predictor layers, linking climate, soils, vegetation, and topography(Steidinger et al., 2019). And Map D (**Fig. 1d)** was derived from a global database on plant mycorrhizal type associations combined with information about dominant plant species across distinct ecoregions and land cover categories derived from satellite(Soudzilovskaia et al., 2019).To better visualize the differences from maps

presented in **Fig.1**, **Fig. 2** shows the differences between each of the ECM fraction maps and Map A, the default mycorrhizal CLM5 configuration(Shi et al., 2016).

The standard deviation of the averaged difference between ECM fraction (%) of each one of the new maps and the default CLM5 map is show in **Fig. 2g**. All three data products agree that the default map in CLM5 overestimates ECM fraction in the boreal regions, as well as drier areas of the world, such as the Atacama, Namibian, Somalian, Mongolian, Sonoran, and Australian deserts. Map C(Steidinger et al., 2019) resembles the default CLM5 map, indicating an alignment of the assumptions that climate variables are the main drivers of global biogeography of forest-tree symbioses and the proposition that fixed values of mycorrhizal associations can be prescribed following PFTs spatial distributions. The three maps disagree in the eastern USA, where Map B(Sulman et al., 2019) indicates Map A(Shi et al., 2016) overestimates ECM fraction, Map C(Steidinger et al., 2019) indicates the opposite, and Map D(Soudzilovskaia et al., 2019) shows small differences. Over eastern Asia the maps also disagree in the sign of changes of ECM fraction with respect to Map A(Shi et al., 2016). Map B(Sulman et al., 2019) shows no particular differences in Northeast China, Map C(Steidinger et al., 2019) indicates Map A(Shi et al., 2016) underestimates ECM fraction, while Map D(Soudzilovskaia et al., 2019) indicates the opposite. In central Europe, Map C(Steidinger et al., 2019) strongly (+40%) revises the default CLM5 ECM fraction upwards for both methodologies, while Maps B(Sulman et al., 2019) and Map D(Soudzilovskaia et al., 2019) show a much smaller positive difference in comparison to Map A(Shi et al., 2016), except for parts of the Alps and parts of the Iberic peninsula. Given that the Map A(Shi et al., 2016) is based on PFT values, the biases to biases in particular PFTs are presented in **Supplementary Fig. S1**.

Although all four maps show high agreement in approximately 60% of the world, some areas present large standard deviation values (> 30%), e.g., Northern Canada and throughout Northern and Eastern Asia, with part of them disagreeing with the sign of change when compared to the original map in CLM5. These areas would benefit from more field measurements and analysis.

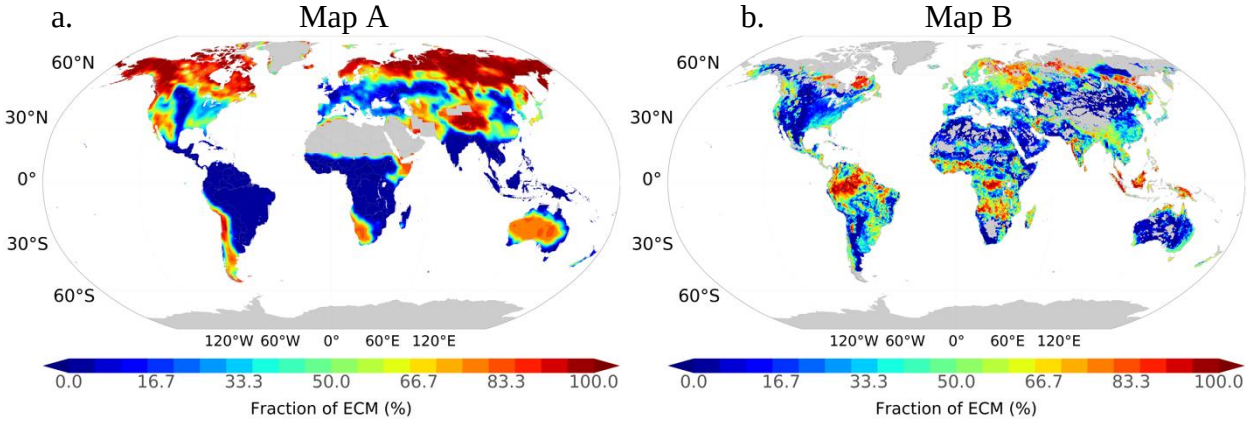

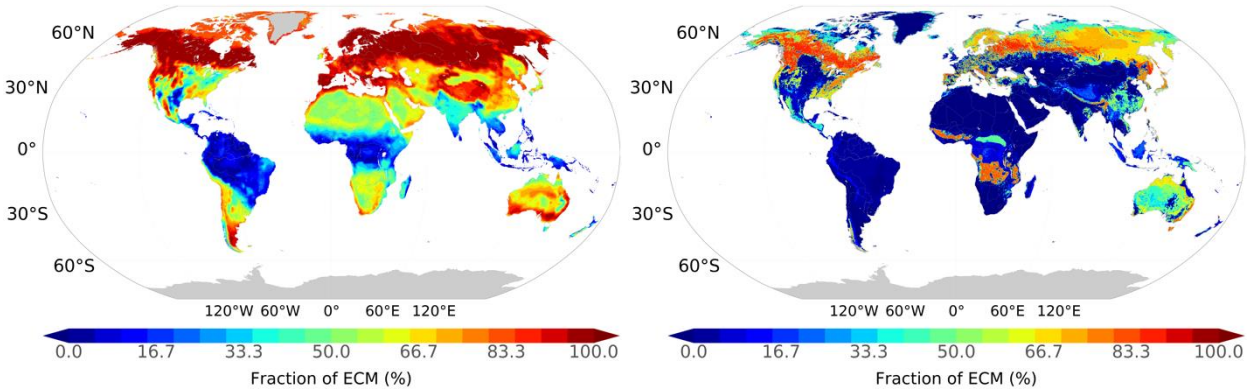

Figure 1. Global spatial distributions of Ectomycorrhizal fraction (%). The remaining fraction is assumed to be arbuscular mycorrhizal. **a.** for ref. (Shi et al., 2016) (Look-up Table x PFTs in 1.9°x2.5°); **b.** ref. (Sulman et al., 2019) (0.17°x0.17°); **c.** ref. (Steidinger et al., 2019) (1.0°x1.0° unmasked); and **d.** ref. (Soudzilovskaia et al., 2019) (0.17°x0.17°).

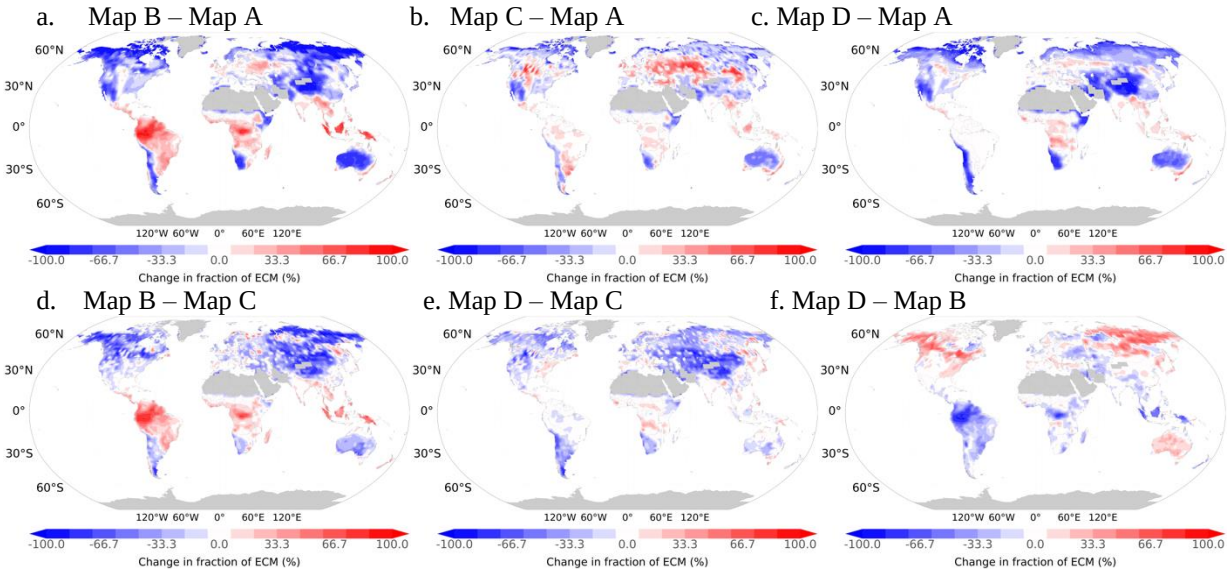

g.

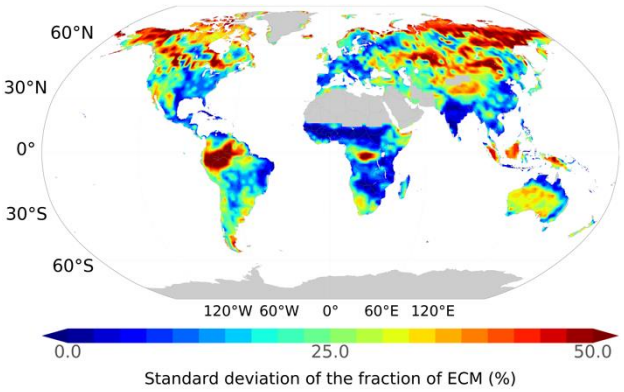

Figure 2. Differences in mycorrhizal distributions among datasets. **a.** Map B (Ref. (Sulman et al., 2019)); **b.** Map C (ref. (Steidinger et al., 2019)); and **c.** Map D (ref. (Soudzilovskaia et al., 2019)) and the base map in CLM5 as in ref. 31 based on PFT values per grid cell. **d.** Map B (ref. (Sulman et al., 2019)); and **e.** Map D (ref. (Soudzilovskaia et al., 2019)) and the Map C (ref. (Steidinger et al., 2019)); **f.** Map D (ref. (Soudzilovskaia et al., 2019)) and the map in Map B (ref. (Sulman et al., 2019)); **g.** standard deviation of all the four maps of ECM fraction.

3.2 Plant symbiotic status impacts on nitrogen uptake pathways

Throughout all runs, the ECM-associated vegetation nitrogen uptake flux (NECM) was the biogeochemical variable most impacted by the inclusion of spatially explicit mycorrhizal status in CLM5, though the other nitrogen uptake pathways were also impacted.

The concept of the Fixation and Uptake of Nitrogen model(Brzostek et al., 2014; J. B. Fisher et al., 2010; R. A. Fisher et al., 2019; Shi et al., 2016) implemented in CLM5 assumes nitrogen uptake requires some expenditure of carbon as energy through different potential sources of nitrogen in the environment. The ratio of carbon expended to nitrogen acquired is referred to as the cost of nitrogen acquisition. There are five different representation of nitrogen acquisition pathways: NECM, AM-associated (NAM), N fixation (NFIX), N retranslocation (NRETRANS), and N non-mycorrhizal (NNONMYC). The sum of all different nitrogen acquisition pathways is the total nitrogen (TOTAL N). **Table 1.0** shows the average values of nitrogen uptake in the period 2000-2010 for each one of the different nitrogen uptake pathways.

Most of the reduction in ECM-associated nitrogen uptake was matched by increases in AM-associated N uptake (**Supplementary Fig. S2**), with a strong signal in the boreal regions. However, changes in N fixation (NFIX) and N retranslocation from leaves (NRETRANS) were also observed. Compared to the default CLM5 simulation, model experiments with the new maps on average estimate more total N fixation (~ 1.6 ± 1.9 %), especially in tropical ecosystems, and less N retranslocation throughout the world (~ -1.1 ± 0.8 %).

Table 1. Average values from 2000 to 2010 of nitrogen uptake by vegetation for each one of the different pathways ($TgNyr^{-1}$) and sum for all new maps and the default one in CLM5.

2000-2010

Pathway	**Reference**	**TRANSIENT – 2000 – 2010**		
(TgNyr-1)	**Map A (CLM5)**	**Map B**	**Map C**	**Map D**
NECM	10.7	10.8	14.8	7.5

NAM	9.9	9.8	8.7	11.8
NFIX	52.0	51.9	52.6	53.8
NRETRANS	92.5	92.4	90.5	91.4
NNONMYC	808.7	805.9	793.0	799.8
TOTAL N	973.7	970.8	959.5	964.4

3.3 Transient runs: the effect of climate change and CO_2 fertilization on nitrogen limitation

On average, the sign of change between the total amount of nitrogen uptake through ECM association between the three updated maps and the default map in CLM5 revises the original ECM nitrogen uptake downwards (**Supplementary Fig. S2 and Fig. S3**). The global total cost of nitrogen uptake was higher for the alternative maps with higher costs over most land areas for the alternative maps (**Supplementary Fig. S4**).

The main areas where carbon costs of nitrogen uptake became more expensive were: Eastern North America, Europe, Southeast Asia, and the tropics for mycorrhizal uptake; tropical and boreal forests for nitrogen fixation; and the tropics for nitrogen retranslocation. Changes in C costs of N acquisition are higher (4.3 ± 4.2% in average globally) in respect to the active pathway associated with mycorrhizal association.

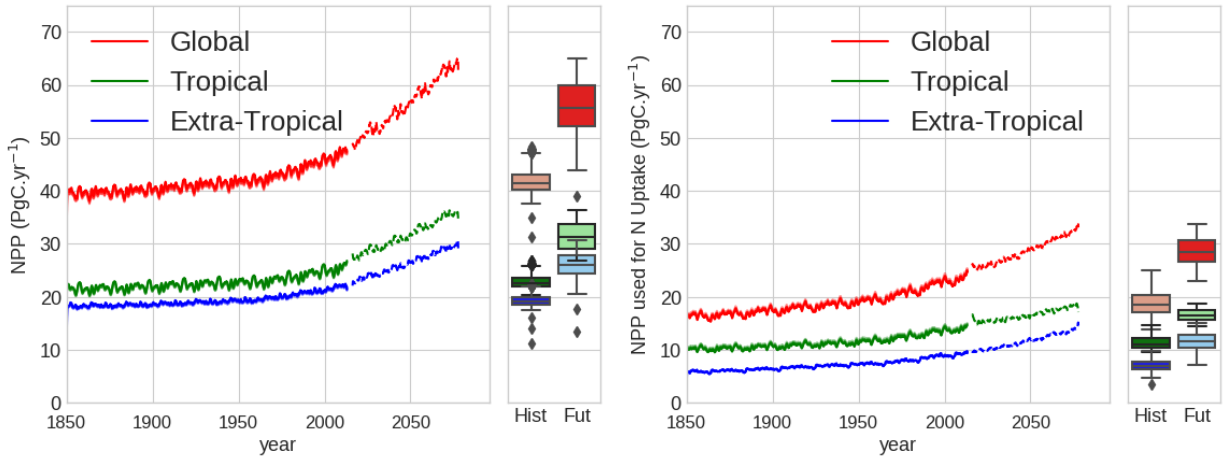

Figure 3. Trend in Net Primary Productivity and usage for nitrogen acquisition **a.** Global total NPP (PgC.yr^{-1}) and **b.** global total carbon cost of nitrogen uptake (NPP_NUPTAKE, PgC.yr^{-1}) for the transient historical run from 1850 to 2010 (continuous) and for the future projection SSP5 with RCP8.5 run from 2015 to 2070 (dashed) with CLM5. Tropical stands for the area of the globe between 23.5°S and 23.5°N. Extra-Tropical is the remaining area of the globe (90°S-23.5°S and 23.5°N-90°N).

In order to determine the climate change effect of nitrogen limitation on plant growth, **Fig. 3** and **Fig. 4** show the global total NPP (PgC.yr^{-1}), global total carbon cost of nitrogen uptake (NPP_NUPTAKE, PgC.yr^{-1}), global plant nitrogen demand (PLANT_NDEMAND,

396 TgN.yr^{-1}), and the global total nitrogen uptake (NUPTAKE, TgN.yr^{-1})**.** Nitrogen demand is
397 calculated as the total N that would be required if all assimilated carbon was allocated according
398 to idealized stoichiometric ratios. The CO_2 fertilization effect, with N deposition and climate
399 variation, increased photosynthetic rates across the globe which are represented by an increase in
400 NPP from 40 PgCyr^{-1} in 1850 to 47.5 PgCyr^{-1} in 2010, or an increase of about 20%. In turn, to
401 support elevated productivity, plants require more nitrogen, leading to an increase in plant
402 nitrogen demand from about 1600 TgN.yr^{-1} in 1850 to 2000 TgN.yr^{-1} in 2010, an increase of
403 about 25%.

404 Although the rates of nitrogen uptake systematically increased in response to a higher
405 nitrogen demand, i.e., NUPTAKE of 800 TgN.yr^{-1} in 1850 to 1000 TgN.yr^{-1} in 2010, the
406 associated carbon costs of nitrogen acquisition increased at a faster rate, growing roughly 40%
407 more expensive in 2010 than in 1850. In terms of the amount of NPP spent in nitrogen
408 acquisition, the values moved from about 7.5% of NPP in 1850 to 11.50% of NPP in 2010. In the
409 transient runs with the default CLM5 Map A, the average growth rate of nitrogen uptake was
410 0.97 TgN.yr^{-2} for the period 1850-2010. In terms of carbon costs, NPP increased at an average
411 rate of 43.14 TgC.yr^{-2} from 1850 to 2010, while the cost of nitrogen acquisition increased at an
412 average rate of 44.38 TgC.yr^{-2} for the same period, an extra 1.24 TgC.yr^{-2}.

413 All transient runs from 1850 to 2010 with the new maps indicated a stronger effect of
414 climate and CO_2 fertilization on nitrogen limitation compared to the default map. Using Map
415 B(Sulman et al., 2019), C(Steidinger et al., 2019), and D(Soudzilovskaia et al., 2019), the
416 average growth rate of nitrogen uptake was 1.00 TgN.yr^{-2}, 0.96 TgN.yr^{-2}, 0.97 TgN.yr^{-2},
417 respectively, while the growth of plant nitrogen demand was 2.77 TgN.yr^{-2}, 2.42 TgN.yr^{-2}, and
418 2.73 TgN.yr^{-2}. In terms of carbon costs, NPP increased at an average rate of 44.17 TgC.yr^{-2} with
419 Map B, 42.79 TgC.yr^{-2} with Map C, and 43.36 TgC.yr^{-2} with Map D. The cost of nitrogen
420 acquisition has increased in a rate of 44.65 TgC.yr^{-2}, 45.16 TgC.yr^{-2}, and 44.46 TgC.yr^{-2} for
421 Maps B, C, and D, respectively.

422 These findings highlight that as estimated by the CLM5 model, not only has plant
423 demand for nitrogen increased at a faster rate than actual nitrogen uptake, but that the carbon
424 costs associated with nitrogen acquisition have increased at a faster rate than the extra carbon
425 gained through the CO_2 fertilization effect. If this pattern continues in the future, it is unlikely
426 that current plant growth rates will be sustained globally.

427

428 **a.** **b.**

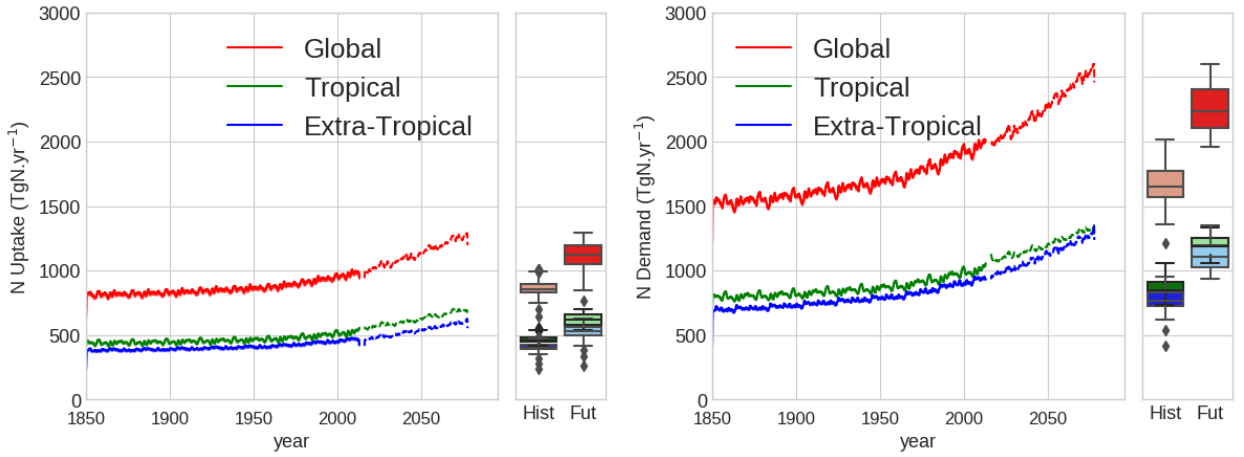

Figure 4. Trend in nitrogen uptake and demand **a.** Global average nitrogen uptake (NUPTAKE, TgN.yr^{-1}); and **b.** global average plant nitrogen demand (PLANT_NDEMAND, TgN.yr^{-1}) for the transient historical run from 1850 to 2010 (continuous) and for the future projection SSP5 RCP8.5 run from 2015 to 2070 (dashed) with CLM5.

Fig. 5 shows the risk of nitrogen limitation (NL), calculated as one minus the ratio of the slope of the linear regression of NPP spent for nitrogen uptake with time to the slope of the linear regression of total NPP with time. NL is normalized from 0 to 1. According to the transient runs from 1850 to 2010 using the default CLM5 Map A, tropical forests have a medium to low risk of being further limited by nitrogen, which is in agreement to some studies that indicate intact ancient tropical forests tend to accumulate and recycle large quantities of nitrogen relative to temperate forests. This can be evidenced by plant and soil nitrogen to phosphorus ratios, by phosphorus limitation of plant growth in some tropical forests, by an abundance of N-fixing plants in the tropics, and by sustained export of bioavailable nitrogen at the ecosystem scale(Hedin et al., 2009). A part of South America, Africa, and Australia, associated with savannas and forest-grassland transition zones present a higher risk of nitrogen limitation to plant growth. Parts of the temperate forests in North America, Europe, and Asia, as well as, northern areas of the planet in the presence of boreal forests present a medium to high risk of nitrogen limitation.

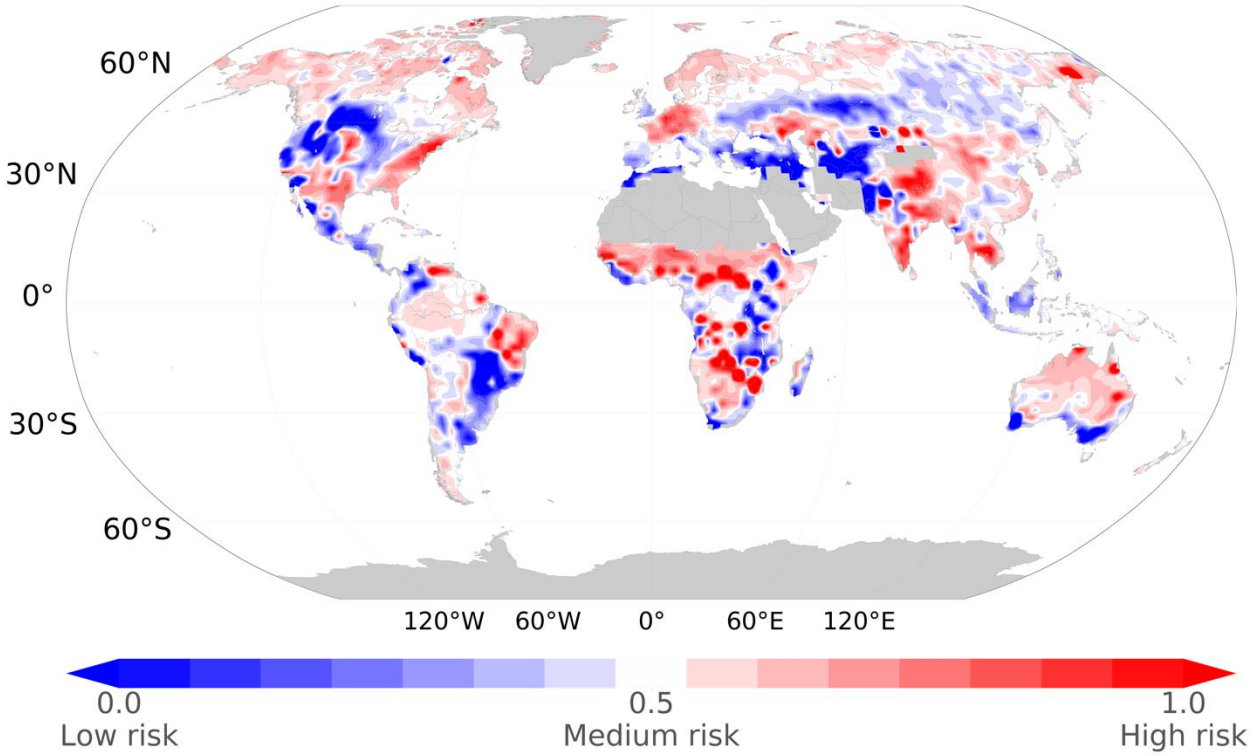

Figure 5. Risk of nitrogen limitation. Areas in red indicate higher risk of nitrogen limitation on NPP, and areas in blue indicate lower risk of nitrogen limitation on NPP.

3.3 The impact of mycorrhizal differences due to climate change

Recent evidence suggests that anthropogenic influences, primarily nitrogen deposition and fire suppression, as well as climate change, have increased AM tree dominance during the past three decades in the eastern United States(Jo et al., 2019). Globally, ref. (Steidinger et al., 2019) presented the only study using the same environment-mycorrhizae relationships for current climate to project potential changes in the symbiotic status of forests in the future, suggesting that projected climate for 2070 reduces the abundance of ECM trees by as much as 10%, with major changes in ECM abundance along the boreal–temperate ecotone (**Fig. 6a**).

Although the magnitude of the time lag between climate change and ecosystem responses is unknown, the predicted decline in ECM trees aligns with previous simulated warming experiments, which have demonstrated that some important ECM hosts decline at the boreal–temperate zones under future climate conditions(Peter B. Reich et al., 2015), and that ECM fungi demonstrated increased responses of mycorrhizal fungal biomass under eCO_2 compared to AM fungi(Dong et al., 2018), as the simulated response in the tropics (**Fig. 6a**).

a. b.

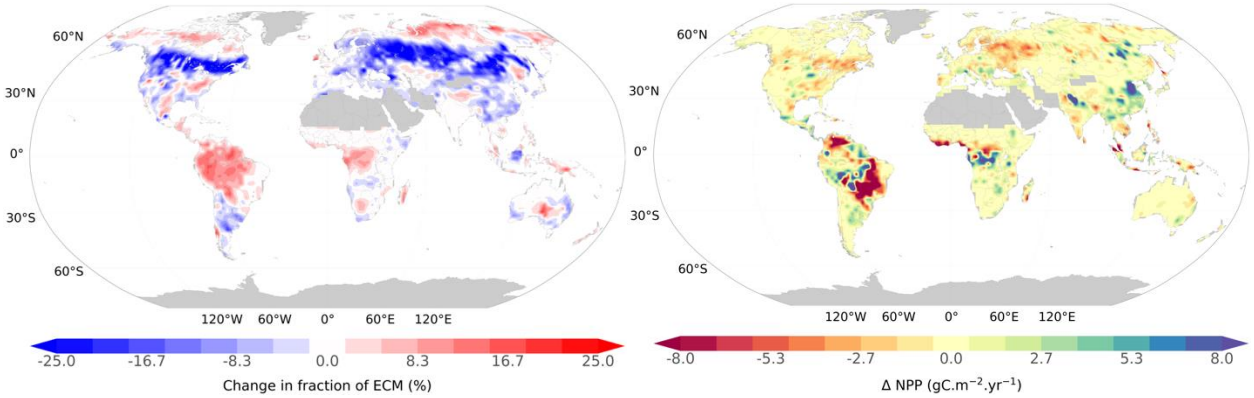

Figure 6. Projected differences in NPP and mycorrhizae driven by climate change **a.** The impact of climate change on ECM fraction (%) derived from ref. (Steidinger et al., 2019) for 2070 following the RCP8.5 with CMIP5 simulations; **b.** Difference in NPP ($gC.m^{-2}.yr^{-1}$) for future simulations (2015-2070) between the projected future map of ref. (Steidinger et al., 2019) generated for the year of 2070 and the present-day map of ref. (Steidinger et al., 2019). The projected runs with CLM5 followed the SSP5 scenario in combination with RCP8.5 climate forcing from CESM, member of CMIP6 simulations.

Although has been reported previously that climate change should impact forest symbiosis, no study has ever evaluated the potential feedback of climate change effects on mycorrhizal distribution onto nitrogen and carbon cycles. The difference in NPP for the period of 2015-2070 between the simulations using the future maps of ectomycorrhizal tree basal area distribution and the simulations using the present-day map of ref. (Steidinger et al., 2019) are shown in **Fig. 6b**.

Large parts of South America especially associated with savannas present the largest negative feedback effects on NPP, followed by areas with boreal forests. The impact over tropical forests and areas in China seem to benefit from a change in plant symbiotic status in the future. Although, these results should be interpreted carefully due to the limitation of the original forest plot training data in those areas of the globe used in ref. (Steidinger et al., 2019), their machine learning model indicates more ECM fungi in the tropics in the future, possibly due to the effect eCO_2 on the tropical climate.

In the SSP5-RCP8.5 runs from 2015 to 2070 with present-day plant symbiotic status map, the growth rate of nitrogen uptake was 4.84 $TgN.yr^{-2}$. In terms of carbon costs, NPP is projected to increase at a rate of 265.54 $TgC.yr^{-2}$, while the carbon cost of nitrogen acquisition is projected to increase at a rate of 130.36 $TgC.yr^{-2}$, an extra 135.18 $TgC.yr^{-1}$.

The feedback effect of climate change on the spatial distribution of plant symbiotic status changes NPP from 58.25 $PgC.yr^{-1}$ to 58.22 $PgC.yr^{-1}$, a negative impact of -23.12 $TgC.yr^{-1}$, and N uptake from 1187.80 $TgN.yr^{-1}$ to 1187.25 $TgN.yr^{-1}$. The projected NPP increase rate with the future plant symbiotic status map is 266.24 $TgC.yr^{-2}$, 0.71 $TgC.yr^{-2}$ faster than the projected NPP without changes in mycorrhizae associations. However, the cost of nitrogen acquisition is projected to increase at a rate of 129.10 $TgC.yr^{-2}$, versus 130.04 $TgC.yr^{-2}$ in the simulations without changes in the spatial distribution of plant symbiotic status. In terms of total NPP globally, these changes are predicted to increase carbon costs of nitrogen acquisition by 582.46 $TgC.yr^{-1}$ amplifying the effect of nutrient limitation on available carbon to plants worldwide.

5 Conclusions

Although the observed distribution of mycorrhizal symbiosis along climatic zones support the link between large-scale plant distributions and soil nutrient availability, the fact that the transition from AM to ECM dominance with increasing latitude follows a parallel transition from phosphorus to nitrogen limitation of plant growth has previously been captured at single site level experiments(McGroddy et al., 2004a; P. B. Reich & Oleksyn, 2004). To overcome the lack of a global spatial representation of mycorrhizal associations, a few studies(Soudzilovskaia et al., 2019; Steidinger et al., 2019; Sulman et al., 2019) have combined a comprehensive quantitative evaluation of mycorrhizae distribution across biomes and continents, and assembled high-resolution digital maps of the global distribution of biomass fractions of different types of mycorrhizae associations.

Nonetheless, while these studies required significant effort to collect and combine extremely large datasets, it is fair to recognize the limits of such global maps. These data products were synthesized through statistical methodologies aggregating areas of the globe strongly underrepresented, e.g., the Amazon and the African continent, with other areas with much more available data, e.g., USA and Europe. Yet, underrepresented areas of the world showed relatively low standard deviation of ECM (%) in comparison to other areas in the Northern North America and Eastern Asia. In our analyses, we show that differences between data products have impacts upon the N and C cycles in the CLM5. This comparison did not aim to determine which map is the most realistic. Rather, we assessed the impact of different mycorrhizal representations in CLM5 to determine signs of changes in the global N and C cycles. On one hand, the CO_2 fertilization effect with a feedback of climate change on mycorrhizal spatial distribution was observed on NPP, especially in South America. On the other hand, the maps coupled with CLM5 did not agree on the total values of N acquisition through different pathways, indicating a source of uncertainty and a need for further validation of these proposed global maps of plant symbiotic status.

Although the transient runs with different spatial representations of plant symbiotic status do not agree in terms of total values of N acquisition through separate pathways, or their relative carbon costs, all experiments agree that the increasing rate of plant N demand is higher than the rate of N uptake. On top of that, the carbon cost of N acquisition also increases faster than NPP itself. Previous studies have also shown a negative CO_2 effect on the nutrient content of crops(Smith & Myers, 2018), as well as a limited effect of CO_2 fertilization on NPP(Zhu et al., 2016), this study also suggests non-sustainable vegetation growth in the future particularly due to N limitation.

Acknowledgments, Samples, and Data

This research was carried out at the Jet Propulsion Laboratory, California Institute of Technology, under a contract with the National Aeronautics and Space Administration. California Institute of Technology. Government sponsorship acknowledged. This material is based upon work supported by the U.S. Department of Energy, Office of Science, Office of Biological and Environmental Research, Terrestrial Ecosystem Science program under Award Numbers DE-SC0008317 and DE-SC0016188. Funding was also provided by the NASA IDS program. Copyright 2020. All rights reserved. We would like to acknowledge high-performance computing support from Cheyenne (NCAR, 2020) provided by NCAR's Computational and Information Systems Laboratory, sponsored by the National Science Foundation.

Data and code availability

A patch file with the modified version of CLM5 and all python scripts used for analyses/plots are available in https://doi.org/10.6084/m9.figshare.12919385.v1.

References

Ali, A. A., Xu, C., Rogers, A., Fisher, R. A., Wullschleger, S. D., Massoud, E. C., et al. (2016). A global scale mechanistic model of photosynthetic capacity (LUNA V1.0). *Geoscientific Model Development*, *9*(2), 587–606. https://doi.org/10.5194/gmd-9-587-2016

Allen, E. B., Allen, M. F., Helm, D. J., Trappe, J. M., Molina, R., & Rincon, E. (1995). Patterns and regulation of mycorrhizal plant and fungal diversity. *Plant and Soil*, *170*(1), 47–62. https://doi.org/10.1007/BF02183054

Allen, K. E., Fisher, J. B., Phillips, R. P., Power, J., & Brzostek, E. R. (2020). Modeling the carbon cost of plant nitrogen and phosphorus uptake across temperate and tropical forests. *Frontiers in Forests and Global Change*. https://doi.org/https://doi.org/10.3389/ffgc.2020.00043

Bailey, R. G. (2014). *Ecoregions: The ecosystem geography of the oceans and continents*. *Ecoregions: The Ecosystem Geography of the Oceans and Continents*. Springer New York. https://doi.org/10.1007/978-1-4939-0524-9

Bartholomé, E., & Belward, A. S. (2005). GLC2000: a new approach to global land cover mapping from Earth observation data. *International Journal of Remote Sensing*. https://doi.org/10.1080/01431160412331291297

Braghiere, R. K., Quaife, T., Black, E., He, L., & Chen, J. M. (2019). Underestimation of Global Photosynthesis in Earth System Models Due to Representation of Vegetation Structure. *Global Biogeochemical Cycles*, *33*(11), 1358–1369. https://doi.org/10.1029/2018GB006135

Brundrett, M. C. (2017). Distribution and Evolution of Mycorrhizal Types and Other Specialised Roots in Australia (pp. 361–394). https://doi.org/10.1007/978-3-319-56363-3_17

Brzostek, E. R., Fisher, J. B., & Phillips, R. P. (2014). Modeling the carbon cost of plant nitrogen acquisition: Mycorrhizal trade-offs and multipath resistance uptake improve predictions of retranslocation. *Journal of Geophysical Research: Biogeosciences*, *119*(8), 1684–1697. https://doi.org/10.1002/2014JG002660

Chen, C., Park, T., Wang, X., Piao, S., Xu, B., Chaturvedi, R. K., et al. (2019). China and India lead in greening of the world through land-use management. *Nature Sustainability*, *2*(2), 122–129. https://doi.org/10.1038/s41893-019-0220-7

Cheng, S. J., Hess, P. G., Wieder, W. R., Thomas, R. Q., Nadelhoffer, K. J., Vira, J., et al. (2019). Decadal fates and impacts of nitrogen additions on temperate forest carbon storage: a data–model comparison. *Biogeosciences*, *16*(13), 2771–2793. https://doi.org/10.5194/bg-

16-2771-2019

Ciais, P., Sabine, C., Bala, G., Bopp, L., Brovkin, V., Canadell, J., et al. (2013). Carbon and Other Biogeochemical Cycles. In T. F. Stocker, D. Qin, G.-K. Plattner, M. Tignor, S. K. Allen, J. Boschung, et al. (Eds.), *Climate Change 2013 - The Physical Science Basis* (pp. 465–570). Cambridge, United Kingdom and New York, NY, USA: Cambridge University Press.

Dong, Y., Wang, Z., Sun, H., Yang, W., & Xu, H. (2018). The Response Patterns of Arbuscular Mycorrhizal and Ectomycorrhizal Symbionts Under Elevated CO2: A Meta-Analysis. *Frontiers in Microbiology*, *9*. https://doi.org/10.3389/fmicb.2018.01248

Drake, J. E., Gallet-Budynek, A., Hofmockel, K. S., Bernhardt, E. S., Billings, S. A., Jackson, R. B., et al. (2011). Increases in the flux of carbon belowground stimulate nitrogen uptake and sustain the long-term enhancement of forest productivity under elevated CO2. *Ecology Letters*, *14*(4), 349–357. https://doi.org/10.1111/j.1461-0248.2011.01593.x

ESA. (2017). CCI Land cover map 2015.

Fisher, J. B., Sitch, S., Malhi, Y., Fisher, R. A., Huntingford, C., & Tan, S.-Y. (2010). Carbon cost of plant nitrogen acquisition: A mechanistic, globally applicable model of plant nitrogen uptake, retranslocation, and fixation. *Global Biogeochemical Cycles*, *24*(1), n/a-n/a. https://doi.org/10.1029/2009GB003621

Fisher, R. A., Wieder, W. R., Sanderson, B. M., Koven, C. D., Oleson, K. W., Xu, C., et al. (2019). Parametric Controls on Vegetation Responses to Biogeochemical Forcing in the CLM5. *Journal of Advances in Modeling Earth Systems*, *11*(9), 2879–2895. https://doi.org/10.1029/2019MS001609

Fleischer, K., Rammig, A., De Kauwe, M. G., Walker, A. P., Domingues, T. F., Fuchslueger, L., et al. (2019). Amazon forest response to CO2 fertilization dependent on plant phosphorus acquisition. *Nature Geoscience*, *12*(9), 736–741. https://doi.org/10.1038/s41561-019-0404-9

Friedlingstein, P., Cox, P., Betts, R., Bopp, L., von Bloh, W., Brovkin, V., et al. (2006). Climate-carbon cycle feedback analysis: Results from the C4MIP model intercomparison. *Journal of Climate*. https://doi.org/10.1175/JCLI3800.1

Friedlingstein, P., Meinshausen, M., Arora, V. K., Jones, C. D., Anav, A., Liddicoat, S. K., & Knutti, R. (2014). Uncertainties in CMIP5 Climate Projections due to Carbon Cycle Feedbacks. *Journal of Climate*, *27*(2), 511–526. https://doi.org/10.1175/JCLI-D-12-00579.1

Friedlingstein, P., Jones, M. W., O'Sullivan, M., Andrew, R. M., Hauck, J., Peters, G. P., et al. (2019). Global Carbon Budget 2019. *Earth System Science Data*, *11*(4), 1783–1838. https://doi.org/10.5194/essd-11-1783-2019

Ghimire, B., Riley, W. J., Koven, C. D., Mu, M., & Randerson, J. T. (2016). Representing leaf and root physiological traits in CLM improves global carbon and nitrogen cycling

predictions. *Journal of Advances in Modeling Earth Systems*. https://doi.org/10.1002/2015MS000538

Goll, D. S., Winkler, A. J., Raddatz, T., Dong, N., Prentice, I. C., Ciais, P., & Brovkin, V. (2017). Carbon–nitrogen interactions in idealized simulations with JSBACH (version 3.10). *Geoscientific Model Development*, *10*(5), 2009–2030. https://doi.org/10.5194/gmd-10-2009-2017

Hedin, L. O., Brookshire, E. N. J., Menge, D. N. L., & Barron, A. R. (2009). The Nitrogen Paradox in Tropical Forest Ecosystems. *Annual Review of Ecology, Evolution, and Systematics*, *40*(1), 613–635. https://doi.org/10.1146/annurev.ecolsys.37.091305.110246

van der Heijden, M. G. A., Martin, F. M., Selosse, M.-A., & Sanders, I. R. (2015). Mycorrhizal ecology and evolution: the past, the present, and the future. *New Phytologist*, *205*(4), 1406–1423. https://doi.org/10.1111/nph.13288

Jo, I., Fei, S., Oswalt, C. M., Domke, G. M., & Phillips, R. P. (2019). Shifts in dominant tree mycorrhizal associations in response to anthropogenic impacts. *Science Advances*, *5*(4), eaav6358. https://doi.org/10.1126/sciadv.aav6358

Keenan, T. F., Prentice, I. C., Canadell, J. G., Williams, C., Wang, H., Raupach, M. R., & Collatz, G. J. (2016). Recent pause in the growth rate of atmospheric CO2 due to enhanced terrestrial carbon uptake. *Nature Communications*. https://doi.org/10.1038/ncomms13428

Kennedy, D., Swenson, S., Oleson, K. W., Lawrence, D. M., Fisher, R., Lola da Costa, A. C., & Gentine, P. (2019). Implementing Plant Hydraulics in the Community Land Model, Version 5. *Journal of Advances in Modeling Earth Systems*, *11*(2), 485–513. https://doi.org/10.1029/2018MS001500

Kim, H. (2017). Global Soil Wetness Project Phase 3 Atmospheric Boundary Conditions (Experiment 1). Data Integration and Analysis System (DIAS). https://doi.org/https://doi.org/10.20783/DIAS.501

Kivlin, S. N., Emery, S. M., & Rudgers, J. A. (2013). Fungal symbionts alter plant responses to global change. *American Journal of Botany*, *100*(7), 1445–1457. https://doi.org/10.3732/ajb.1200558

Kolus, H. R., Huntzinger, D. N., Schwalm, C. R., Fisher, J. B., McKay, N., Fang, Y., et al. (2019). Land carbon models underestimate the severity and duration of drought's impact on plant productivity. *Scientific Reports*, *9*(1), 2758. https://doi.org/10.1038/s41598-019-39373-1

Kriegler, E., Bauer, N., Popp, A., Humpenöder, F., Leimbach, M., Strefler, J., et al. (2017). Fossil-fueled development (SSP5): An energy and resource intensive scenario for the 21st century. *Global Environmental Change*, *42*, 297–315. https://doi.org/10.1016/j.gloenvcha.2016.05.015

Lawrence, D. M., Hurtt, G. C., Arneth, A., Brovkin, V., Calvin, K. V., Jones, A. D., et al. (2016).

The Land Use Model Intercomparison Project (LUMIP) contribution to CMIP6: rationale and experimental design. *Geoscientific Model Development*, *9*(9), 2973–2998. https://doi.org/10.5194/gmd-9-2973-2016

Lawrence, D. M., Fisher, R. A., Koven, C. D., Oleson, K. W., Swenson, S. C., Bonan, G., et al. (2019). The Community Land Model Version 5: Description of New Features, Benchmarking, and Impact of Forcing Uncertainty. *Journal of Advances in Modeling Earth Systems*, *11*(12), 4245–4287. https://doi.org/10.1029/2018MS001583

McGroddy, M. E., Daufresne, T., & Hedin, L. O. (2004a). Scaling of C:N:P stoichiometry in forests worldwide: implications of terrestrial redfield-type ratios. *Ecology*, *85*(9), 2390–2401. https://doi.org/10.1890/03-0351

McGroddy, M. E., Daufresne, T., & Hedin, L. O. (2004b). SCALING OF C:N:P STOICHIOMETRY IN FORESTS WORLDWIDE: IMPLICATIONS OF TERRESTRIAL REDFIELD-TYPE RATIOS. *Ecology*, *85*(9), 2390–2401. https://doi.org/10.1890/03-0351

Menzel, A., Hempel, S., Manceur, A. M., Götzenberger, L., Moora, M., Rillig, M. C., et al. (2016). Distribution patterns of arbuscular mycorrhizal and non-mycorrhizal plant species in Germany. *Perspectives in Plant Ecology, Evolution and Systematics*, *21*, 78–88. https://doi.org/10.1016/j.ppees.2016.06.002

NCAR. (2019). CLM5 Documentation Release, 337.

NCAR. (2020). CHEYENNE. https://doi.org/10.5065/D6RX99HX

Norby, R. J., De Kauwe, M. G., Walker, A. P., Werner, C., Zaehle, S., & Zak, D. R. (2017). Comment on “Mycorrhizal association as a primary control of the CO 2 fertilization effect.” *Science*, *355*(6323), 358.2-358. https://doi.org/10.1126/science.aai7976

O’Neill, B. C., Tebaldi, C., Van Vuuren, D. P., Eyring, V., Friedlingstein, P., Hurtt, G., et al. (2016). The Scenario Model Intercomparison Project (ScenarioMIP) for CMIP6. *Geoscientific Model Development*, *9*(9), 3461–3482. https://doi.org/10.5194/gmd-9-3461-2016

Öpik, M., Vanatoa, A., Vanatoa, E., Moora, M., Davison, J., Kalwij, J. M., et al. (2010). The online database MaarjAM reveals global and ecosystemic distribution patterns in arbuscular mycorrhizal fungi (Glomeromycota). *New Phytologist*, *188*(1), 223–241. https://doi.org/10.1111/j.1469-8137.2010.03334.x

Orwin, K. H., Kirschbaum, M. U. F., St John, M. G., & Dickie, I. A. (2011). Organic nutrient uptake by mycorrhizal fungi enhances ecosystem carbon storage: a model-based assessment. *Ecology Letters*, *14*(5), 493–502. https://doi.org/10.1111/j.1461-0248.2011.01611.x

Phillips, R. P., Brzostek, E., & Midgley, M. G. (2013). The mycorrhizal-associated nutrient economy: a new framework for predicting carbon-nutrient couplings in temperate forests. *New Phytologist*, *199*(1), 41–51. https://doi.org/10.1111/nph.12221

694 Read, D. J. (1991). Mycorrhizas in ecosystems. *Experientia*, *47*(4), 376–391.
695 https://doi.org/10.1007/BF01972080

696 Reich, P. B., & Oleksyn, J. (2004). Global patterns of plant leaf N and P in relation to
697 temperature and latitude. *Proceedings of the National Academy of Sciences*, *101*(30),
698 11001–11006. https://doi.org/10.1073/pnas.0403588101

699 Reich, Peter B., Sendall, K. M., Rice, K., Rich, R. L., Stefanski, A., Hobbie, S. E., &
700 Montgomery, R. A. (2015). Geographic range predicts photosynthetic and growth response
701 to warming in co-occurring tree species. *Nature Climate Change*, *5*(2), 148–152.
702 https://doi.org/10.1038/nclimate2497

703 Riahi, K., van Vuuren, D. P., Kriegler, E., Edmonds, J., O'Neill, B. C., Fujimori, S., et al.
704 (2017). The Shared Socioeconomic Pathways and their energy, land use, and greenhouse
705 gas emissions implications: An overview. *Global Environmental Change*, *42*, 153–168.
706 https://doi.org/10.1016/j.gloenvcha.2016.05.009

707 Schimel, D., Stephens, B. B., & Fisher, J. B. (2015). Effect of increasing CO 2 on the terrestrial
708 carbon cycle. *Proceedings of the National Academy of Sciences*, *112*(2), 436–441.
709 https://doi.org/10.1073/pnas.1407302112

710 Shi, M., Fisher, J. B., Brzostek, E. R., & Phillips, R. P. (2016). Carbon cost of plant nitrogen
711 acquisition: global carbon cycle impact from an improved plant nitrogen cycle in the
712 Community Land Model. *Global Change Biology*, *22*(3), 1299–1314.
713 https://doi.org/10.1111/gcb.13131

714 Smith, M. R., & Myers, S. S. (2018). Impact of anthropogenic CO2 emissions on global human
715 nutrition. *Nature Climate Change*, *8*(9), 834–839. https://doi.org/10.1038/s41558-018-0253-
716 3

717 Soudzilovskaia, N. A., van Bodegom, P. M., Terrer, C., Zelfde, M. van't, McCallum, I., Luke
718 McCormack, M., et al. (2019). Global mycorrhizal plant distribution linked to terrestrial
719 carbon stocks. *Nature Communications*, *10*(1), 5077. https://doi.org/10.1038/s41467-019-
720 13019-2

721 Steidinger, B. S., Crowther, T. W., Liang, J., Van Nuland, M. E., Werner, G. D. A., Reich, P. B.,
722 et al. (2019). Climatic controls of decomposition drive the global biogeography of forest-
723 tree symbioses. *Nature*, *569*(7756), 404–408. https://doi.org/10.1038/s41586-019-1128-0

724 Sulman, B. N., Brzostek, E. R., Medici, C., Shevliakova, E., Menge, D. N. L., & Phillips, R. P.
725 (2017). Feedbacks between plant N demand and rhizosphere priming depend on type of
726 mycorrhizal association. *Ecology Letters*, *20*(8), 1043–1053.
727 https://doi.org/10.1111/ele.12802

728 Sulman, B. N., Shevliakova, E., Brzostek, E. R., Kivlin, S. N., Malyshev, S., Menge, D. N. L., &
729 Zhang, X. (2019). Diverse Mycorrhizal Associations Enhance Terrestrial C Storage in a
730 Global Model. *Global Biogeochemical Cycles*, *33*(4), 501–523.
731 https://doi.org/10.1029/2018GB005973

Swaty, R., Michael, H. M., Deckert, R., & Gehring, C. A. (2016). Mapping the potential mycorrhizal associations of the conterminous United States of America. *Fungal Ecology*, *24*, 139–147. https://doi.org/10.1016/j.funeco.2016.05.005

Tedersoo, L., Bahram, M., Põlme, S., Kõljalg, U., Yorou, N. S., Wijesundera, R., et al. (2014). Global diversity and geography of soil fungi. *Science*, *346*(6213), 1256688. https://doi.org/10.1126/science.1256688

Terrer, C., Vicca, S., Hungate, B. A., Phillips, R. P., & Prentice, I. C. (2016). Mycorrhizal association as a primary control of the CO 2 fertilization effect. *Science*, *353*(6294), 72–74. https://doi.org/10.1126/science.aaf4610

Terrer, C., Vicca, S., Stocker, B. D., Hungate, B. A., Phillips, R. P., Reich, P. B., et al. (2018). Ecosystem responses to elevated CO 2 governed by plant-soil interactions and the cost of nitrogen acquisition. *New Phytologist*, *217*(2), 507–522. https://doi.org/10.1111/nph.14872

Terrer, C., Jackson, R. B., Prentice, I. C., Keenan, T. F., Kaiser, C., Vicca, S., et al. (2019). Nitrogen and phosphorus constrain the CO2 fertilization of global plant biomass. *Nature Climate Change*, *9*(9), 684–689. https://doi.org/10.1038/s41558-019-0545-2

Trenberth, K. E., Dai, A., van der Schrier, G., Jones, P. D., Barichivich, J., Briffa, K. R., & Sheffield, J. (2014). Global warming and changes in drought. *Nature Climate Change*, *4*(1), 17–22. https://doi.org/10.1038/nclimate2067

Wang, Y. P., Law, R. M., & Pak, B. (2010). A global model of carbon, nitrogen and phosphorus cycles for the terrestrial biosphere. *Biogeosciences*, *7*(7), 2261–2282. https://doi.org/10.5194/bg-7-2261-2010

Waring, B. G., Adams, R., Branco, S., & Powers, J. S. (2016). Scale-dependent variation in nitrogen cycling and soil fungal communities along gradients of forest composition and age in regenerating tropical dry forests. *New Phytologist*, *209*(2), 845–854. https://doi.org/10.1111/nph.13654

Wieder, W. R., Cleveland, C. C., Smith, W. K., & Todd-Brown, K. (2015). Future productivity and carbon storage limited by terrestrial nutrient availability. *Nature Geoscience*, *8*(6), 441–444. https://doi.org/10.1038/ngeo2413

Wieder, W. R., Lawrence, D. M., Fisher, R. A., Bonan, G. B., Cheng, S. J., Goodale, C. L., et al. (2019). Beyond static benchmarking: Using experimental manipulations to evaluate land model assumptions. *Global Biogeochemical Cycles*. https://doi.org/10.1029/2018GB006141

Xu, C., Fisher, R., Wullschleger, S. D., Wilson, C. J., Cai, M., & McDowell, N. G. (2012). Toward a mechanistic modeling of nitrogen limitation on vegetation dynamics. *PLoS ONE*, *7*(5), 1–11. https://doi.org/10.1371/journal.pone.0037914

Zaehle, S., Friedlingstein, P., & Friend, A. D. (2010). Terrestrial nitrogen feedbacks may accelerate future climate change. *Geophysical Research Letters*, *37*(1), n/a-n/a. https://doi.org/10.1029/2009GL041345

Zaehle, S., Jones, C. D., Houlton, B., Lamarque, J.-F., & Robertson, E. (2015). Nitrogen Availability Reduces CMIP5 Projections of Twenty-First-Century Land Carbon Uptake. *Journal of Climate*, *28*(6), 2494–2511. https://doi.org/10.1175/JCLI-D-13-00776.1

Zhang, Y., Song, C., Band, L. E., & Sun, G. (2019). No Proportional Increase of Terrestrial Gross Carbon Sequestration From the Greening Earth. *Journal of Geophysical Research: Biogeosciences*, 2018JG004917. https://doi.org/10.1029/2018JG004917

Zhu, Z., Piao, S., Myneni, R. B., Huang, M., Zeng, Z., Canadell, J. G., et al. (2016). Greening of the Earth and its drivers. *Nature Climate Change*. https://doi.org/10.1038/NCLIMATE3004